AIP | Journal of Applied Physics

Non-periodicity of peak-to-peak distances in x-ray diffraction spectrums from perfect superlattices

I. Sankowska, J. Z. Domagala, O. M. Yefanov, A. Jasik, J. Kubacka-Traczyk et al.

Citation: J. Appl. Phys. **113**, 064302 (2013); doi: 10.1063/1.4790712
View online: http://dx.doi.org/10.1063/1.4790712
View Table of Contents: http://jap.aip.org/resource/1/JAPIAU/v113/i6
Published by the American Institute of Physics.

Related Articles

High mobility half-metallicity in the (LaMnO3)2/(SrTiO3)8 superlattice
Appl. Phys. Lett. 102, 042401 (2013)

Strain effects on magnetic characteristics of ultrathin La0.7Sr0.3MnO3 in epitaxial La0.7Sr0.3MnO3/BaTiO3 superlattices
J. Appl. Phys. 112, 123919 (2012)

Radiation tolerance characterization of dual band InAs/GaSb type-II strain-layer superlattice pBp detectors using 63 MeV protons
Appl. Phys. Lett. 101, 251108 (2012)

Nanostructured thermoelectric cobalt oxide by exfoliation/restacking route
J. Appl. Phys. 112, 113705 (2012)

Strain effect in PbTiO3/PbZr0.2Ti0.8O3 superlattices: From polydomain to monodomain structures
J. Appl. Phys. 112, 114102 (2012)

Additional information on J. Appl. Phys.

Journal Homepage: http://jap.aip.org/
Journal Information: http://jap.aip.org/about/about_the_journal
Top downloads: http://jap.aip.org/features/most_downloaded
Information for Authors: http://jap.aip.org/authors

ADVERTISEMENT

Downloaded 09 Feb 2013 to 129.174.21.5. Redistribution subject to AIP license or copyright; see http://jap.aip.org/about/rights_and_permissions

JOURNAL OF APPLIED PHYSICS **113**, 064302 (2013)

Non-periodicity of peak-to-peak distances in x-ray diffraction spectrums from perfect superlattices

I. Sankowska,[1] J. Z. Domagala,[1,2] O. M. Yefanov,[3,4] A. Jasik,[1] J. Kubacka-Traczyk,[1] K. Regiński,[1] and O. H. Seeck[4]

[1]*Institute of Electron Technology, Al. Lotników 32/46, Warsaw 02-668, Poland*
[2]*Institute of Physics, Polish Academy of Sciences, Al. Lotników 32/46, Warsaw 02-668, Poland*
[3]*V. Lashkarev Institute of Semiconductor Physics, 45 Nauky Ave., Kiev 03680, Ukraine*
[4]*Deutsches Electronen-Synchrotron (DESY), Notkestraße 85, Hamburg D-22607, Germany*

(Received 20 November 2012; accepted 24 January 2013; published online 8 February 2013)

X-ray diffraction investigations of type II InAs/GaSb superlattice on a GaSb(001) substrate are presented. The wide range of diffraction angles ($2\theta/\omega$ scans) covering 002 and 004 reflections was examined at Petra III synchrotron. The angular region between 002 and 004 reflections was the most interesting part of the measured diffraction profile. In this region, a non-coincidence of superlattice satellite peaks belonging to these two reflections is observed. The multiple-beam dynamical diffraction approach was used for correct simulation of the observed diffraction profile.
© *2013 American Institute of Physics*. [http://dx.doi.org/10.1063/1.4790712]

I. INTRODUCTION

The development of the growth techniques has resulted in semiconductor structures with high crystalline perfection. This is important for the electronic devices based on superlattices (SLs) which consist of tens or hundreds periods formed by several layers each. High or perfect quality of structures is obtained when the thickness and chemical composition of individual layers in different periods are kept constant during the whole growth process. To control the structural quality, x-ray diffraction and reflection methods are usually used.[1–3] The resolution of such diffraction measurements is determined through the range of the measured reciprocal space, which is usually proportional to the range of diffraction angles. The limiting factor for the increasing the resolution is the fact that the intensity of scattered x-rays drops as q^2–q^4. Therefore to increase the resolution twice, eight times more photons are needed. For this, the synchrotron radiation is much more attractive than the conventional laboratory x-ray sources.

The quality of SLs in a wide range of diffraction angles covering regions between 00*l* reflections (*l*–natural number, consistent with selection rules for SL crystallographic structure) has been investigated by Schuster[4] and Podorov.[5] In the Ref. 4, the AlAs/GaAs superlattice on GaAs substrate was characterized. The synchrotron measurements showed that the satellite peaks belonging to the 002 and 004 reflections did not coincide. Unfortunately, theoretical calculation of the diffraction profile for wide angular range was not performed to describe the observed phenomenon. The InSb/InGaSb/InSb/InAs superlattice was grown on GaSb substrate and was investigated by Podorov.[5] For this periodic structure, the authors assumed that two different reflections coincide perfectly—there are no shifts between 002 SL and 004 SL family peaks. However, the experimental data were insufficient to observe the angular range of interest. This is due to the low intensities of higher order SL peaks for both 002 and 004 reflections when the data were measured by a laboratory diffractometer. For the simulation, the authors proposed to use a theoretical approach based on two distorted waves. Unfortunately, the diffraction profile was simulated in a very wide angular range from 10 to 60 degree. Such plot makes it difficult to conclude about the coincidence of high-order satellites peaks for two different reflections. Theoretical prediction of diffraction profiles taken for modified superlattice due to the thickness change of constituent layers and interfaces in a period have been presented in Ref. 6.

In our paper, we present the wide-angle x-ray diffraction measurement of type II InAs/GaSb superlattice grown on a GaSb(001) substrate. The measurements were performed in symmetrical Bragg geometry for the range of the incidence angles from 6 to 28 degree utilizing the x-rays with 22.117 keV energy. In this range, two GaSb reflections, namely 002 and 004, were observed. The part of the diffraction curve in which the SL satellite peaks from two reflections overlap is the most interesting for further analysis. To simulate correctly such experimental data, the usual approach of two strong waves is not applicable. In such geometrical conditions, several reciprocal lattice nodes simultaneously take part in the formation of a diffraction pattern due to the enhancement of the signal along the truncation rod. Therefore, the simulation of diffraction profile was performed using the *N*-beam dynamical diffraction theory, taking simultaneously into account three reciprocal nodes—000, 002, and 004. This simulation successfully described the measured data.

II. EXPERIMENT AND RESULTS

The investigated multilayer periodic heterostructure was grown by molecular beam epitaxy (MBE) in a Riber 32P machine equipped with RHEED system (10 kV) to monitor crystallographic surface features. Conventional effusion cells

 © 2013 American Institute of Physics

Downloaded 09 Feb 2013 to 129.174.21.5. Redistribution subject to AIP license or copyright; see http://jap.aip.org/about/rights_and_permissions

were used for group III elements, whereas valved cracking cells were intended for group V elements. The sample was grown on so called "epi-ready" undoped GaSb(001) substrate. The miscut angle between substrate lattice and substrate surface was experimentally checked and equals about 0.2 degree. Prior to a run growth, the water vapour was desorbed from the substrate surface at the temperature of 350 °C for 15 minutes. In the growth chamber, the wafer temperature was increased up to about 530 °C for the native oxide desorption. To improve the surface purity, further wafer heating was continued under Sb-flux. The annealing temperature was kept constant at 550 °C during 2 minutes. The GaSb buffer layer was grown at 530 °C and beam equivalent pressure (BEP) ratio of about 2.5. The growth rate of GaSb and InAs layers was 0.5 monolayer/second (ML/s). The growth processes of InAs/GaSb superlattice were carried out as follows. Growth of GaSb was followed by an arsenic soak to form an interface (IF) between GaSb and InAs. Switching from InAs to GaSb, an antimony soak was used for preferential formation of InSb-like bonds. The optimized soak times and group V fluxes were used to form sharp interfaces. The superlattice formed by 30 periods was characterized by high resolution x-ray diffraction (HRXRD). The thicknesses of layers and interfaces have been obtained from simulation and are as follows: GaSb 2.90 nm (9.5 ML), IF InSb 0.14 nm (0.4 ML), InAs 2.38 nm (7.9 ML), and IF $InAs_{0.29}Sb_{0.71}$ 0.16 nm (0.5 ML).

The HRXRD measurement was performed using laboratory diffractometer PANalytical X'Pert PRO in the following configuration: the Cu $K\alpha_1$ ($\lambda \sim 1.54056$ Å) radiation, the hybrid $4 \times$ Ge(400) monochromator, and three bounce Ge(220) analyzer. The HRXRD measurement in wide angular range was performed at the High Resolution Diffraction Beamline P08[7] at the 3-th generation x-ray synchrotron source PETRA III, HASYLAB at the research center DESY. The six-circle diffractometer NZD-3 (Kohzu) was used. The x-ray beam, of energy 22.117 keV (0.56058 Å), was first monochromatized using cooled by liquid nitrogen double Si(111) monochromator followed by double Si(511) monochromator. This setup allows achieving high q-resolution and very good higher harmonic suppression. The proportional NaI-detector (Cyberstar Scintillation detector, FMB-Oxford) was used for measuring the diffracted intensity.

The GaSb 004 diffraction pattern of InAs/GaSb superlattice obtained using laboratory diffractometer is shown in Fig. 1(a). This structure is lattice matched. It means that a perpendicular average lattice constant of SL is the same as a perpendicular lattice constant of GaSb(001) substrate, Fig. 1(b). It can also be seen that the satellite peaks up to fifth order are observed. Unfortunately, the intensity of higher ordered peaks is very low. Therefore, it is not possible to observe the angular region in which satellite peaks from symmetrical 002 and 004 reflections overlap. For that reason, the synchrotron radiation, with much higher monochromatic flux, was used. Even for 002 reflection, which is quasiforbidden, the signal intensity is high and easy to detect. The wide angle diffraction pattern measured at synchrotron source is shown in Fig. 2(a).

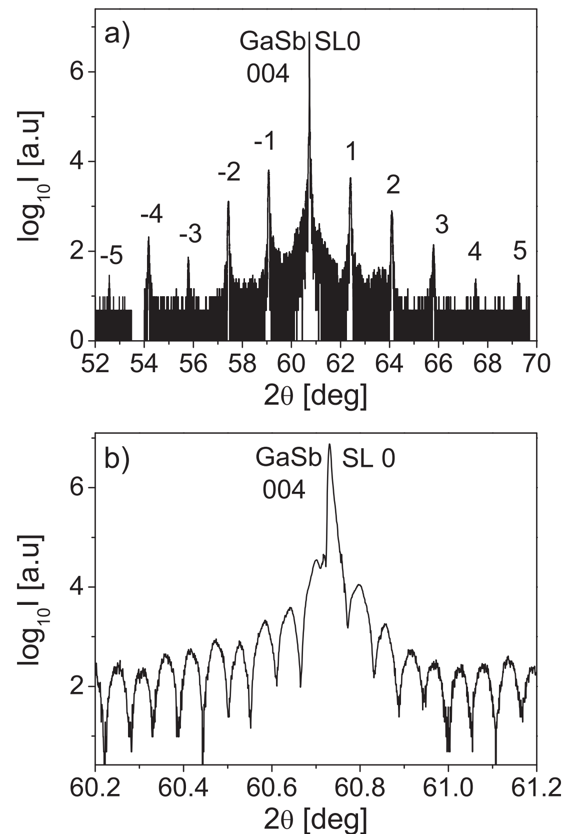

FIG. 1. (a) Experimental diffraction curve of periodic InAs/GaSb structure measured around the GaSb 004 reflection ($\lambda \sim 1.54056$ Å, laboratory source). (b) The 0-th satellite peak coincides with the substrate Bragg peak—the perpendicular lattice mismatch is 0 ppm.

Due to the high flux of synchrotron radiation, two satellite groups belonging to the 002 and 004 reflections are observed in the diffraction profile. The GaSb 002 and GaSb 004 substrate reflections are the most intensive peaks. Besides the substrate reflections the numerous of the satellite peaks up to the tenth order are presented. The detailed view of a diffraction profile in the angular range from 14 degree to 18 degree is shown in Fig. 2(b). In this region, the overlapping of the satellite peaks belonging to the families 002 and 004 reflection is observed. The peaks from two families do not coincide. Such discrepancy of the SL peaks may wrongly suggest that the periodicity of the structure is not maintained. Furthermore, the additional satellite peaks which were theoretically predicted in Ref. 6 have not been noticed. It is worth noting that this effect of the non-coincidence of the satellite peaks that we observed was also seen by us in the case of diffraction measurement of InAs/GaSb superlattice with two controlled interfaces. The period of this SL is consisted of the following layers and interfaces: GaSb 9.6 ML, InSb IF 1.4 ML, InAs 10.1 ML, GaAs IF 0.4 ML.

The overlapping of satellite peaks for different reflections will be explained below based on the concept of the reciprocal space (RS). It is widely accepted that for perfect superlattice distance between all reciprocal lattice points (RLPs) in RS should be equal, Fig. 3(a). In this figure, triangles represent 002 superlattice family RLPs, whereas the circles represent 004 superlattice family RLPs. Our experimental data can be represented by Fig. 3(b). In this figure,

Downloaded 09 Feb 2013 to 129.174.21.5. Redistribution subject to AIP license or copyright; see http://jap.aip.org/about/rights_and_permissions

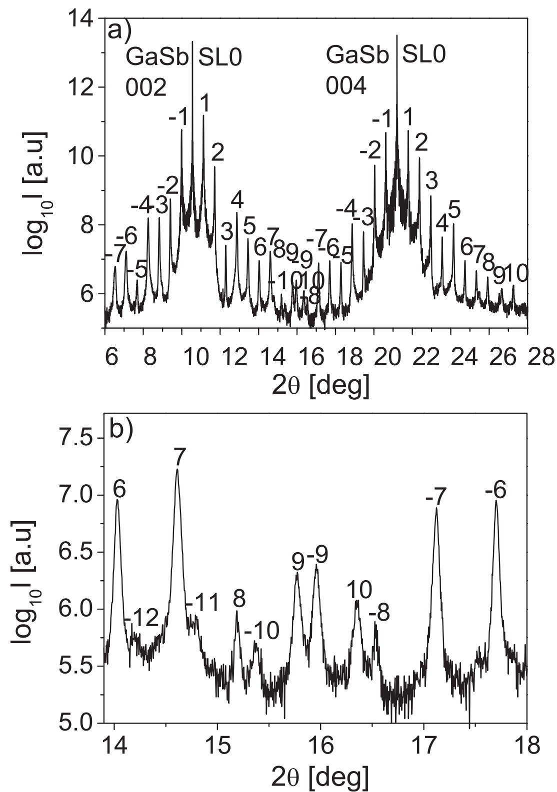

FIG. 2. (a) Experimental diffraction pattern (synchrotron source) of periodic InAs/GaSb structure measured around the GaSb 002 and 004 reflections; (b) Detailed view of a diffraction pattern in the range between 002 and 004 GaSb reflections in which the overlap of satellite peaks is observed. Negative and positive numbers indicate left and right satellite peaks from family of specific reflection.

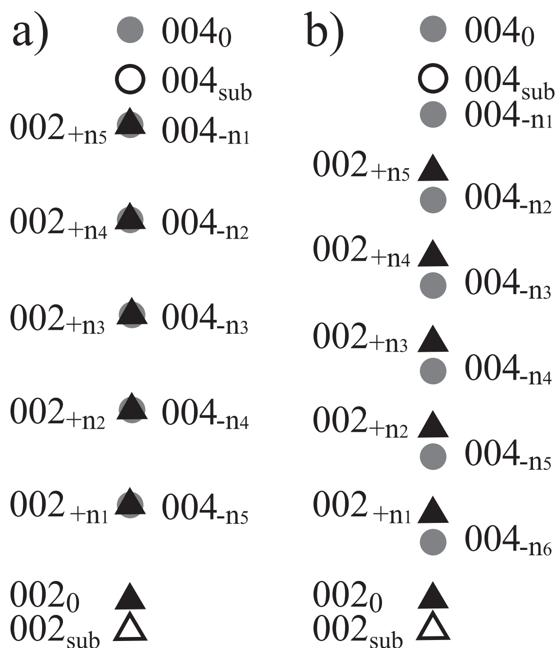

FIG. 3. Reciprocal lattice points for superlattice structures for which 002 and 004 satellite peaks overlap (a) and do not overlap (b). Full triangles represent SL satellites around reflection 002; full circles represent SL satellites around reflection 004. Open triangles and circles correspond to the substrate peaks.

two different distances between a circle and two neighbour triangles are observed. However, the distance q_{SL} between reciprocal lattice points belonging to one of the families 002 or 004 reflection is the same (between circles or between triangles in Fig. 3(b)). These two cases presented in Fig. 3 can be observed experimentally, but the case presented in Fig. 3(a) is a specific situation from Fig. 3(b). The condition for coincidence of 002 and 004 reciprocal lattice points will be presented below.

The relaxation state of the structure was checked by measuring the symmetrical and asymmetrical reciprocal space maps in four experimental geometries, when edge of the sample parallel to the one of the families of {110} directions, was perpendicular to the axis of the diffractometer. No relaxation was observed. Example of the experimental symmetrical and asymmetrical reciprocal space maps is presented in Fig. 4.

The period of our superlattice consists of GaSb and InAs layers and InSb-like interfaces. Therefore, the period thickness d_{SL} of such SL is equal:

$$d_{SL} = \Big(N_1 a_{GaSb} + N_2 a_{InSb\,IF} + N_3 a_{InAs} + N_4 a_{InAs(x)Sb(1-x)\,IF}\Big) \cdot 0.5, \qquad (1)$$

where $N_{1(3)}$ is the number of monolayers of GaSb (InAs) layer, $a_{GaSb\ (InAs)}$ is the perpendicular lattice constant of GaSb (InAs) layer, $N_{2(4)}$ is the number of monolayers of InSb ($InAs_{(x)}Sb_{(1-x)}$)-like interface, and $a_{InSb\ IF,(InAs(x)Sb(1-x)\ IF)}$ is the perpendicular lattice constant of InSb ($InAs_{(x)}Sb_{(1-x)}$ IF)-like interface.

Another feature of SL structure is existence of so called "zero" SL peaks for the families of the 00*l* RLP ($l = 2, 4, 6$). The average lattice constant corresponding to the 0-th peak is equal:

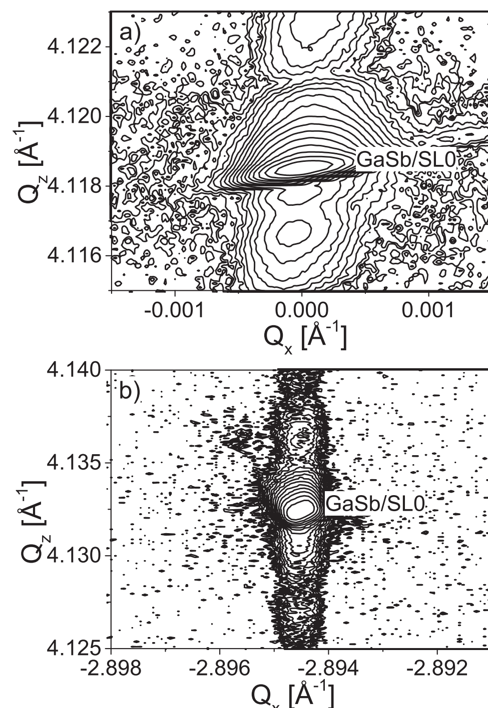

FIG. 4. Symmetrical (a) and asymmetrical (b) reciprocal space maps.

Downloaded 09 Feb 2013 to 129.174.21.5. Redistribution subject to AIP license or copyright; see http://jap.aip.org/about/rights_and_permissions

$$\langle a_{SL}\rangle = \frac{\left(N_1 a_{GaSb} + N_2 a_{InSb\,IF} + N_3 a_{InAs} + N_4 a_{InAs(x)Sb(1-x)\,IF}\right)\cdot 0.5}{N_1+N_2+N_3+N_4}. \quad (2)$$

From Eqs. (1) and (2), we obtained:

$$\langle a_{SL}\rangle = \frac{d_{SL}}{N_1+N_2+N_3+N_4}. \quad (3)$$

In the reciprocal space, the distances between 00l superlattice RLPs family are express by

$$\frac{1}{d_{SL}} = Q^{00l}_{n(i)} - Q^{00l}_{n(i-1)} = q_{SL}, \quad (4)$$

where $Q^{00l}_{n(i)}$ and $Q^{00l}_{n(i-1)}$ is the positions of the $n_{\rm i}$ and $n_{(\rm i-1)}$ superlattice reciprocal lattice points belonging to 00l reflection, and q_{SL} is the distance between the superlattice RLPs for 00l reflection.

The distance between the 0-th RLPs for each family ($\Delta Q_{SL(0)}$), in our case 002 and 004 families, equals

$$\frac{1}{\langle a_{SL}\rangle} = Q^{004}_{SL(0)} - Q^{002}_{SL(0)} = \Delta Q_{SL(0)}, \quad (5)$$

$Q^{002}_{SL(0)}$ and $Q^{004}_{SL(0)}$—positions of the 0-th reciprocal lattice points belonging to 002 and 004 reflections, respectively.

If we use Eqs. (4) and (5) into Eq. (3), we obtain that

$$\Delta Q_{SL(0)} = (N_1+N_2+N_3+N_4)q_{SL}. \quad (6)$$

The Eq. (6) is the condition for determining when the 002 and 004 reciprocal lattice points will coincide. The perfect overlapping of 002 and 004 RLPs presented in Fig. 3(a) will be observed, when the $\Delta Q_{SL(0)}$ equals the total multiplicity of q_{SL}. So this means that the $(N_1+N_2+N_3+N_4)$ must be an integer, otherwise the situation from Fig. 3(b) will be arise. The sample is characterised by $\sum N_i = (9.5+0.4+7.9+0.5) = 18.3$ and for that we observe non-coincidence of satellite peaks belonging to the SL families of 002 and 004 reflections.

III. THEORETICAL CALCULATION

The non-coincidence of satellite peaks in the area far from the Bragg reflections can be explained using a kinematical approach and even using the simple geometrical approach—as was performed in paragraph II. However to correctly simulate the whole range of the scanned reciprocal space within a single framework, the dynamical theory is required. In this paragraph, we present the theoretical approach that can be used for correct simulation of the diffraction curve in a wide angular range. This approach is based on dynamical diffraction theory and takes into account simultaneous influence of several sets of crystal planes (or reciprocal lattice nodes) on the diffraction pattern. This is usually referred to as N-beam (or multiple beam) diffraction,[8] where N is the number of the reciprocal lattice nodes including the node 000. In such a framework, the propagation equation for each n-th wave-field, derived from Maxwell equations, is written as[9]

$$(k^2_{h_n}-1)\vec{E}_{h_n} = (\vec{k}_{h_n}\cdot\vec{E}_{h_n})\vec{k}_{h_n} + K^2\sum_{m=0}^{N-1}\chi_{h_n-h_m}\vec{E}_{h_m}\quad, \quad (7)$$

where $\vec{k}_{h_n}$ is the wave-vectors in medium ($K-$in vacuum) corresponding to reciprocal lattice vectors $\vec{h}_n$, $\vec{E}_{h_n}$ is the electrical fields, and $\chi_{h_n-h_m}$ is the Fourier components of polarizability.

The vector equation can be transformed to set of scalar equations by decomposition of all wave-vectors and wave-fields into Cartesian components (see Ref. 9 for details).

To find the amplitudes of the diffracted waves, boundary conditions, which correspond to continuity of components E_t, D_n, H_t, and B_n, are used[9]

$$\begin{aligned} E_t &= const, \; D_n = const,\\ H_t &= const, \; B_n = const, \end{aligned} \quad (8)$$

where n and t subscripts correspond to normal and tangential components of the fields, respectively.

The Eqs. (7) and (8) could be used for the multilayered structures as follows. First the propagation, Eq. (7) is solved for each layer for determination of the wave-vectors and wave-fields. Then the boundary conditions between layers and at both sides of the whole structure are applied to derive all diffracted waves. The easiest way to describe boundary conditions for multilayered structures with arbitrary layers is using matrix approach similar to Parrat's formula.[10] Then the final solution for the whole structure consisting of M layers can be written as follows:

$$c_M = (S_M)^{-1}S_{M-1}F_{M-1}(S_{M-1})^{-1}\cdots(S_2)^{-1}S_1F_1c_1, \quad (9)$$

where c is the matrixes of reflection/transmission coefficients, S is the matrixes of the waves inside each layer, and F is the matrixes corresponding to propagation through the layer.

Detailed description of this algorithm with the definition of all matrices can be found in Ref. 11. This algorithm extends the multiple-beam approach developed for a single crystal slab[9] to the case of an arbitrary multilayered structure and therefore incorporates its main advantages. The main features of the used N-beam dynamical diffraction approach are

- a propagation equation and boundary conditions are solved without simplifications,
- suitable for any geometry (Bragg, Laue, Brag-Laue),
- the model can be 3D in reciprocal and 1D in real space,
- covers the whole angular range,

Downloaded 09 Feb 2013 to 129.174.21.5. Redistribution subject to AIP license or copyright; see http://jap.aip.org/about/rights_and_permissions

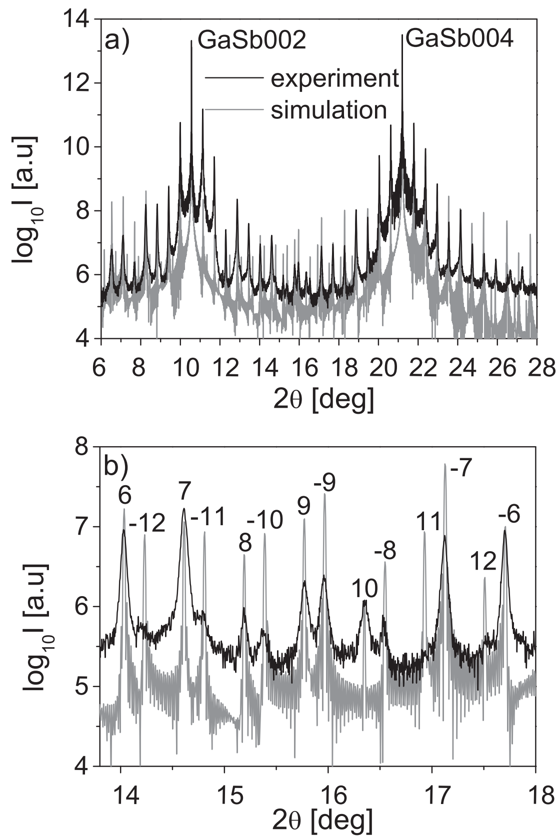

FIG. 5. Simulated diffraction pattern from present theory (dashed curve) compared with experimental one (solid line).

- precise calculation of any polarization with information on diffracted and reflected beams polarization,
- no principal limitation on quantity of reciprocal lattice points considered simultaneously,
- no limitations on layers thickness.

Using this strategy, the diffraction profile shown in Fig. 5 was simulated for the InAs/GaSb superlattice described in the experimental part. To simulate correctly, the intensity distribution in the angular range between 002 and 004 Bragg peaks, including the region around the peaks, simultaneous diffraction of three strong reflections 000, 002, and 004 was calculated.

Due to the presence of strong truncation rods from both 002 and 004 reflections in the angular range between the Bragg peaks, strong interference of the two independent set of satellites is noted. All main features of the experimental profile are very well reproduced by the simulated diffraction pattern.

IV. CONCLUSION

In summary, synchrotron radiation diffraction measurements of a type II InAs/GaSb superlattice covering a wide range of diffraction angles have been presented. The most intriguing part of the measured diffraction profile was the region between 002 and 004 reflections. In this region, the satellite peaks corresponding to 002 and 004 substrate reflections do not coincide. We explained nature of the phenomena and we have shown in a simple way that there is a special condition for which the perfect coinciding of SL peaks for two symmetric reflections can be observed. We think that the results shown in this paper are important for proper interpretation of diffraction curves from SL. Furthermore to correctly simulate the diffraction pattern of the multilayered structure in a wide angular range, the dynamical multiple-beam diffraction theory was used. This approach allows us to take into account simultaneous influence of three strong reflections 000, 002, and 004 on the formation of a x-ray diffraction. The comparison of the simulated profile with the measured one demonstrated a very good agreement of the satellite peaks positions.

ACKNOWLEDGMENTS

The authors would like to thank J. Kaniewski for helpful cooperation. This work was partially supported by the Polish Ministry of Science and Higher Education under projects No. PBZ- MNiSW 02/I/2007 and NCBiR No. 02 0023 06.

[1] D. K. Bowen and B. K. Tanner, *High Resolution X-ray Diffractometry and Topography* (Taylor & Francis Ltd, London, 1998).
[2] V. Holy, U. Pietsch, and T. Baumbach, *High Resolution X-ray Scattering*, 2nd ed. (Springer-Verlag, New York, 2004).
[3] P. F. Fewster, *X-ray Scattering from Semiconductors*, 2nd ed. (Imperial College Press, London, 2003).
[4] M. Schuster, A. Lessmann, A. Munkholm, S. Brennan, G. Materlik, and H. Reichert, J. Phys. D: Appl. Phys. **28**, A206 (1995).
[5] S. G. Podorov, N. N. Faleev, K. M. Pavlov, D. M. Paganin, S. A. Stepanov, and E. Förster, J. Appl. Cryst. **39**, 652 (2006).
[6] S. K. Kim, C. H. Chang, Y. P. Lee, and Y. M. Koo, J. Appl. Phys. **77**(1), 423 (1995).
[7] O. H. Seeck, C. Deiter, K. Pflaum, F. Bertram, A. Beerlink, H. Franz, J. Horbach, H. Schulte-Schrepping, B. M. Murphy, M. Greve, and O. Magnussen, J. Synchrotron. Rad. **19**, 30 (2012).
[8] S. L. Chang, *Multiple Diffraction of X-rays in Crystals* (Springer-Verlag, Berlin, 1984).
[9] Y. P. Stetsko and S.-L. Chang, Acta Cryst. A **53**, 28 (1997).
[10] L. G. Parratt, Phys. Rev. **95**, 359 (1954).
[11] O. M. Yefanov, V. P. Kladko, V. F. Machulin, and V. B. Molodkin, *Dynamical X-rays Diffraction in Multilayered Structures*, (Naukova Dumka, Kiev, 2008).

Downloaded 09 Feb 2013 to 129.174.21.5. Redistribution subject to AIP license or copyright; see http://jap.aip.org/about/rights_and_permissions